August 27-31, 2023
FLORENCE - ITALY
16th International Conference on Wind Engineering
ICWE 16

Effects of vortex convection on generation of negative peak pressures on bluff body

Xincong Wang [1], Qiusheng Li [1,2,*], Bin Lu [1], Ming Li [3]

[1]*Department of Architecture and Civil Engineering, City University of Hong Kong, Hong Kong*
[2]*Architecture and Civil Engineering Research Center, City University of Hong Kong Shenzhen Research Institute, Shenzhen, China, bcqsli@cityu.edu.hk*
[3] *Wind Eng Key Laboratory of Sichuan Province, Southwest Jiaotong University, Chengdu, China*

SUMMARY:
The effects of vortex convection on negative peak pressures on a blunt plate under a separation bubble are investigated with Large Eddy Simulation (LES). Synchronized sampling of the wind pressures on and the velocity fields around the plate is used to investigate the effects of vortex convection on extreme pressure fluctuations. The vortex dynamics of convection, dissipation, and merging is visualized using flow field snapshots of streamlines. It is found that a negative peak pressure usually occurs when the vortex core is right beneath/above the observation point. The occurrence can be brought forward or delayed by vortex dissipation or vortex merging, respectively. The contribution of vortex convection on pressure fluctuations is further confirmed by pressure correlation analysis. The convection speed and spatial scale of the related vortex structure are investigated. The present study provides insights to the generation of negative peak pressures and valuable information for flow control and wind-resistant design.

Keywords: negative peak pressures, vortex convection, bluff body aerodynamics

1. INTRODUCTION

Negative peak pressures are known as the main cause of local damages of buildings, such as the roof failure of low-rise buildings and the façade damage of tall buildings. It is commonly conjectured that the pressure fluctuations are related to vortex convection. However, the research on the specific effects of vortex dynamics on extreme pressure fluctuations on bluff bodies is limited. This study aims at investigating the generation of negative peak pressures on a blunt plate surface within a separated and reattaching flow, with special attention to the validation and investigation of the effects of vortex dynamics on extreme pressure fluctuations on bluff body.

2. NUMERICAL MODEL AND VALIDATION

2.1. Numerical Model

A sketch of the computation domain and boundary conditions is displayed in Fig. 1. The depth (D) and breadth (B) of the blunt plate are 0.1 m and 0.5 m, respectively. The plate is modelled with perfectly sharp edges. The dimensions of the computation domain are set as $180\,D \times 101\,D \times 5\,D$ ($L_x \times L_y \times L_z$). The incoming smooth flow is set to be normal to the blunt plate. The inlet velocity U is 6 m/s, resulting a depth-based Reynolds number Re_D of 40,000. Large Eddy Simulation (LES) is conducted to solve the incompressible Navier-Stokes equations. The code package OpenFOAM is used in this study.

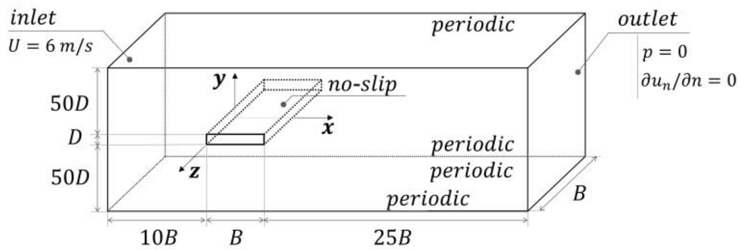

Figure 1. Computation domain and boundary conditions

2.2. Validation

The mean and standard deviation of the drag coefficient (C_D) and the lift coefficient (C_L), the Strouhal number (S_t), and the reattachment length (X_r) are compared with those of Wind Tunnel (WT) and Computational Fluid Dynamics (CFD) studies on 5:1 blunt plate. The results have shown a good agreement (Table 1). The pressure coefficients along the centerline of the bottom plate surface also compare reasonably with those of previous studies as shown in Figs. 2-3.

Table 1. Comparisons of bulk parameters

Sources	Approach	Re_D	t-avg (C_D)	t-avg (C_L)	t-std(C_L)	S_t	X_r
Wu et al. (2020)	WT	53,600	1.1	~0	-	0.12	-
Zhang and Xu (2020)	LES	40,000	0.97	-	0.27	0.12	4.14 D
Present study	LES	40,000	0.97	-0.001	0.25	0.13	4.15 D

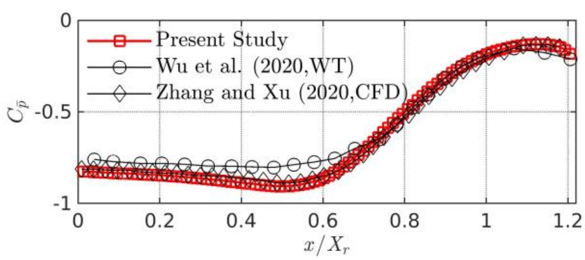

Figure 2. Mean wind pressure coefficients

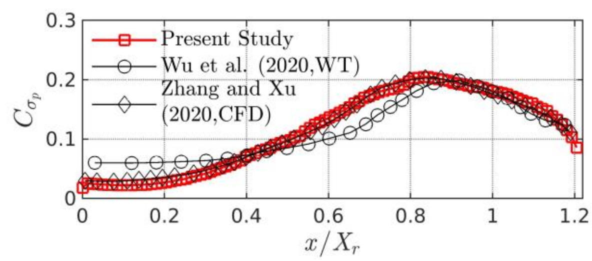

Figure 3. R.M.S. wind pressure coefficients

3. EFFECTS OF VORTEX DYNAMICS ON EXTREME PRESSURE FLUCTUATIONS

3.1. Extreme Negative Peak Pressures

Extreme negative peak pressures are defined with a threshold of $p < \bar{p} - 3\sigma_p$, where $\bar{p}$ is the mean and σ_p is the standard deviation of pressure signals. Normalized upcrossing frequencies (Saathoff and Melbourne, 1997) for a set of streamwise locations along the centreline of the bottom plate surface are shown in Fig. 4. The position where the extreme negative peak pressures occur most frequently is found at $x = 0.265\,X_r = 1.1\,D$ (Figs. 4-5).

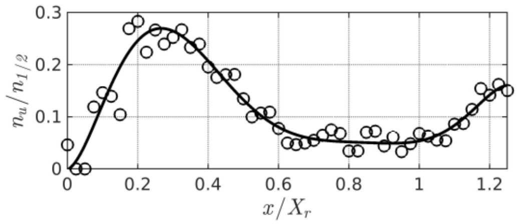

Figure 4. Normalized upcrossing frequencies

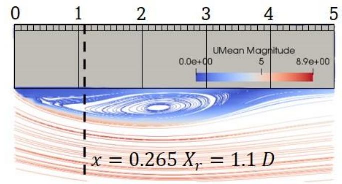

Figure 5. Time-averaged velocity field

3.2. Vortex Convection

Pressure series at three observation points and the simultaneous velocity field snapshots are displayed in Fig. 6. It can be found in Fig. 6c that a vortex convects downstream from the leading edge with a continuous increase of the spatial scale until the location around x=1.4 D. At x=1.4 D, vortex dissipation (T=57.72-57.96) and vortex merging (T=91.44-92.28) may happen. Correspondingly, the occurrence of large suctions at the upstream points (Point A at x=0.8 D and Point B at x=1.1 D) is highly related with vortex passing. The negative peak pressures always occur at the instant that the vortex core passing by. Whereas the occurrence of negative peak pressures at Point C (at x=1.4 D) is brought forward due to vortex dissipation within T=57.72-57.96 and delayed due to vortex merging within T=91.80-92.04, respectively. The time-averaged convection speed and spatial scale of the related vortex can be estimated from the snapshots as 0.43 U_∞ and 0.85 D, respectively.

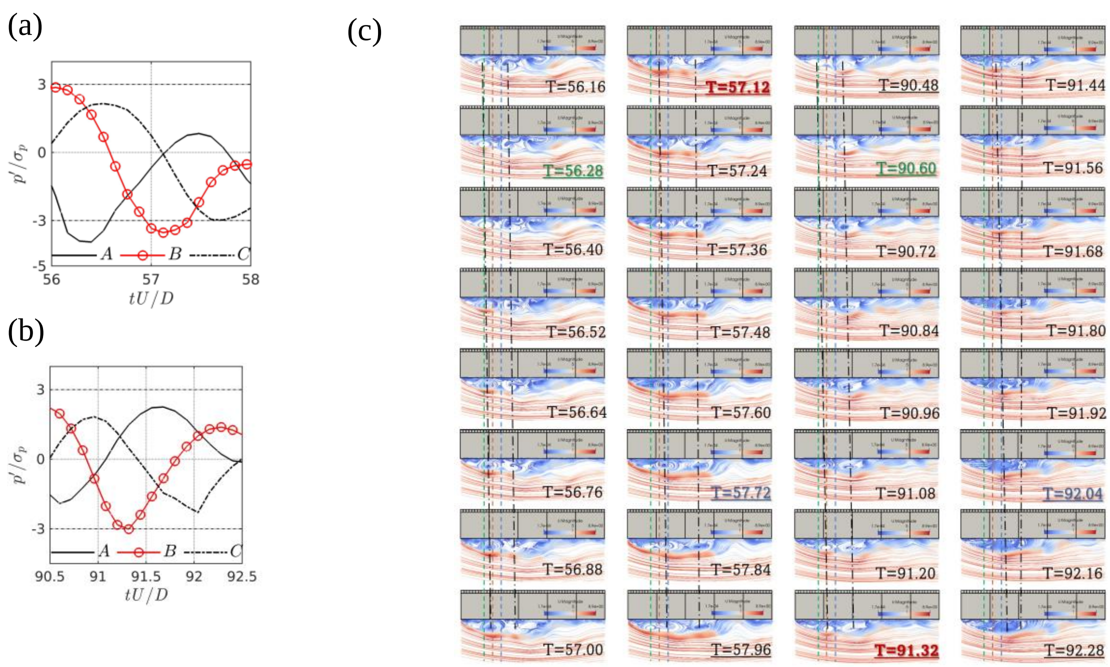

Figure 6. Vortex convection

(Points A, B, C: points along the central line of the bottom surface; Dash lines: x=0.8 D (green, Point A), x=1.1 D (red, Point B), and x=1.4 D (blue, Point C); Dotted lines: vortex cores.)

3.2. Pressure Correlations

A pressure correlation analysis is performed to extend the findings for individual cases in 3.1 into the general time domain (Fig. 7). The observation point is fixed at point B at $x = 1.1\,D$. Other two points (A at $x = 0.8\,D$ and C at $x = 1.4\,D$) are selected as reference points. Pressure correlations R_{pp} are calculated with $R_{pp} = cov(p_n(t), p_B(t+\tau))/\sigma_n\sigma_B$, where n denotes the indices of the reference points, τ is the time lag between two pressure series. A dash line connecting peaks across the subplots is shown in Fig. 7, which indicates a vortex convecting from A to C successively. The time-averaged convection speed and spatial scale of the vortex structure can be estimated from Fig. 7 as 0.5 U_∞ and 0.9 D, respectively. Both values compare reasonably with that estimated from Fig. 6 considering the limited samples. It confirms the contribution of vortex convection to extreme pressure fluctuations, which further lead to the generation of negative peak pressures.

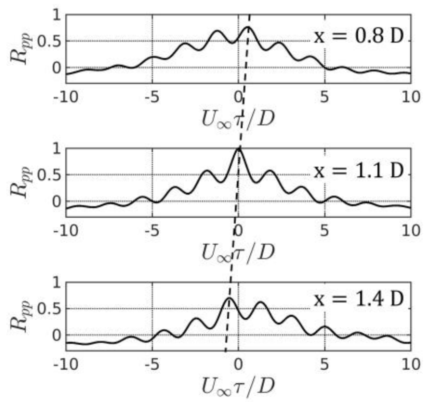

Figure 7. Pressure correlations

4. CONCLUSIONS

The synchronized sampling strategy of the wind pressures and velocity fields was applied to explore the effects of vortex dynamics on the pressure fluctuations on a blunt plate. It was found that the negative peak pressures usually occur at a position while a vortex core passing by. The occurrence can be brought forward due to vortex dissipation and delayed when vortex merging happens. The contribution of vortex convection on pressure fluctuations was then confirmed using pressure correlation analysis.

ACKNOWLEDGEMENTS

The work described in this paper was fully supported by a grant from the Fundamental Research Program of Shenzhen Municipality (Project No: JCYJ20170818094653701).

REFERENCES

Saathoff, P. J. and Melbourne, W. H., 1997. Effects of free-stream turbulence on surface pressure fluctuations in a separation bubble. Journal of Fluid Mechanics 337, 1-24.

Schmid, P. J., 2010. Dynamic mode decomposition of numerical and experimental data. Journal of Fluid Mechanics 656, 5-28.

Wu, B., Li, S. P., Li, K., and Zhang, L. L., 2020. Numerical and experimental studies on the aerodynamics of a 5:1 rectangular cylinder at angles of attack. Journal of Wind Engineering and Industrial Aerodynamics 199, 104097.

Zhang, Z. B. and Xu, F. Y., 2020. Spanwise length and mesh resolution effects on simulated flow around a 5:1 rectangular cylinder. Journal of Wind Engineering and Industrial Aerodynamics 202, 104186.